Supplementary Information

In vitro metabolism of azaspiracid-1–3 with a hepatopancreatic fraction from blue mussels (*Mytilus edulis*)

Morten Sandvik, Christopher O. Miles, Kjersti L. E. Løvberg, Fedor Kryuchkov, Elliott J. Wright, Elizabeth M. Mudge, Jane Kilcoyne, and Ingunn A. Samdal

Table of contents

Table S1 is available as an Excel spreadsheet, and shows the accurate masses observed, mass errors, and potential structures of structurally diagnostic product ions observed during LC–HRMS and LC–HRMS/MS (method A) of metabolites in this study.

In vitro metabolism of AZA1–3 in blue mussel hepatopancreatic fraction

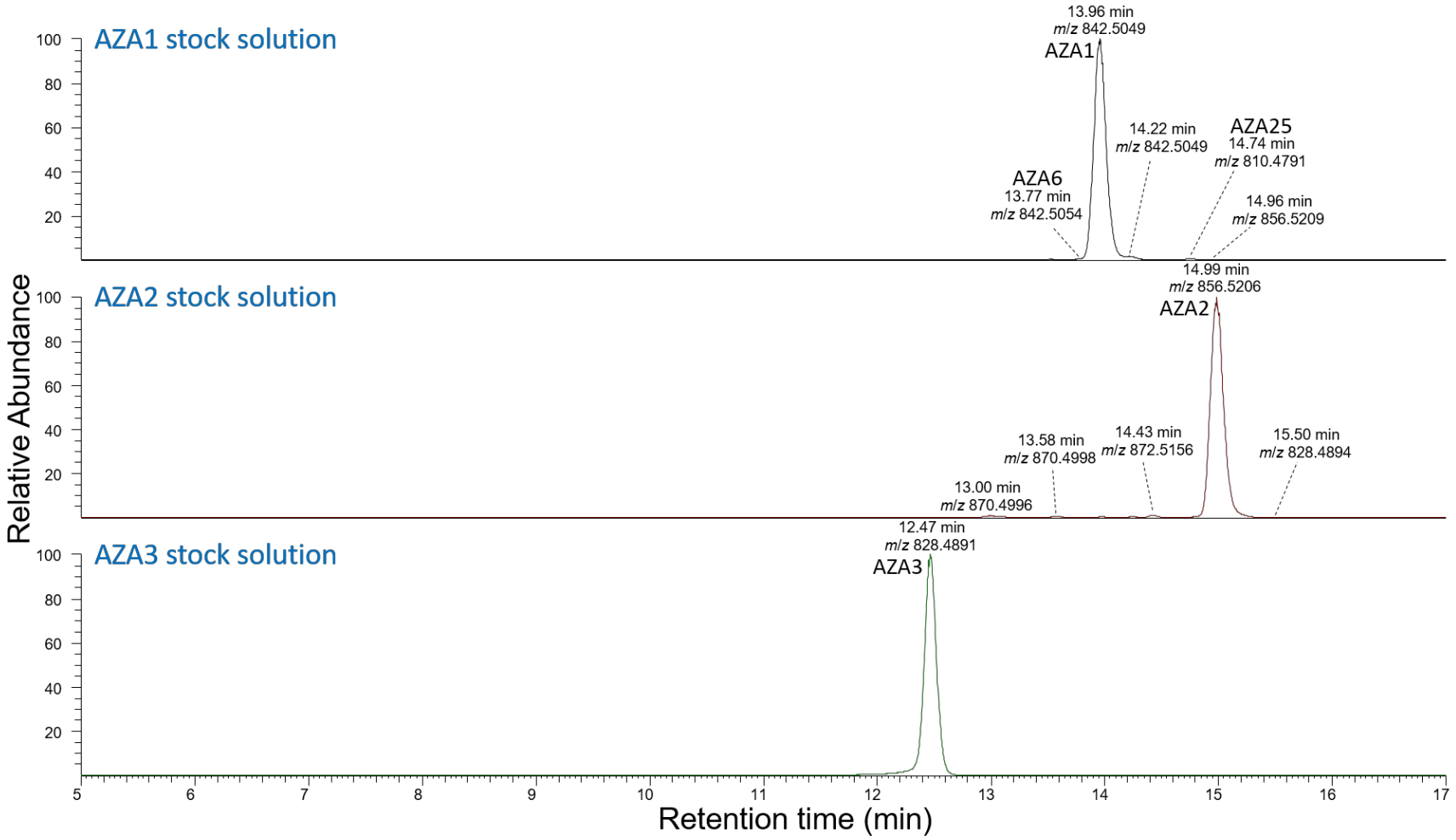

Figure S1. LC–HRMS (method A) base peak chromatograms (*m*/*z* 790–920) of the stock solutions of top, AZA1; middle, AZA2, and; bottom, AZA3. These stock solutions were used for the *in vitro* metabolism studies with the hepatopancreatic fractions.

In vitro metabolism of AZA1–3 in blue mussel hepatopancreatic fraction

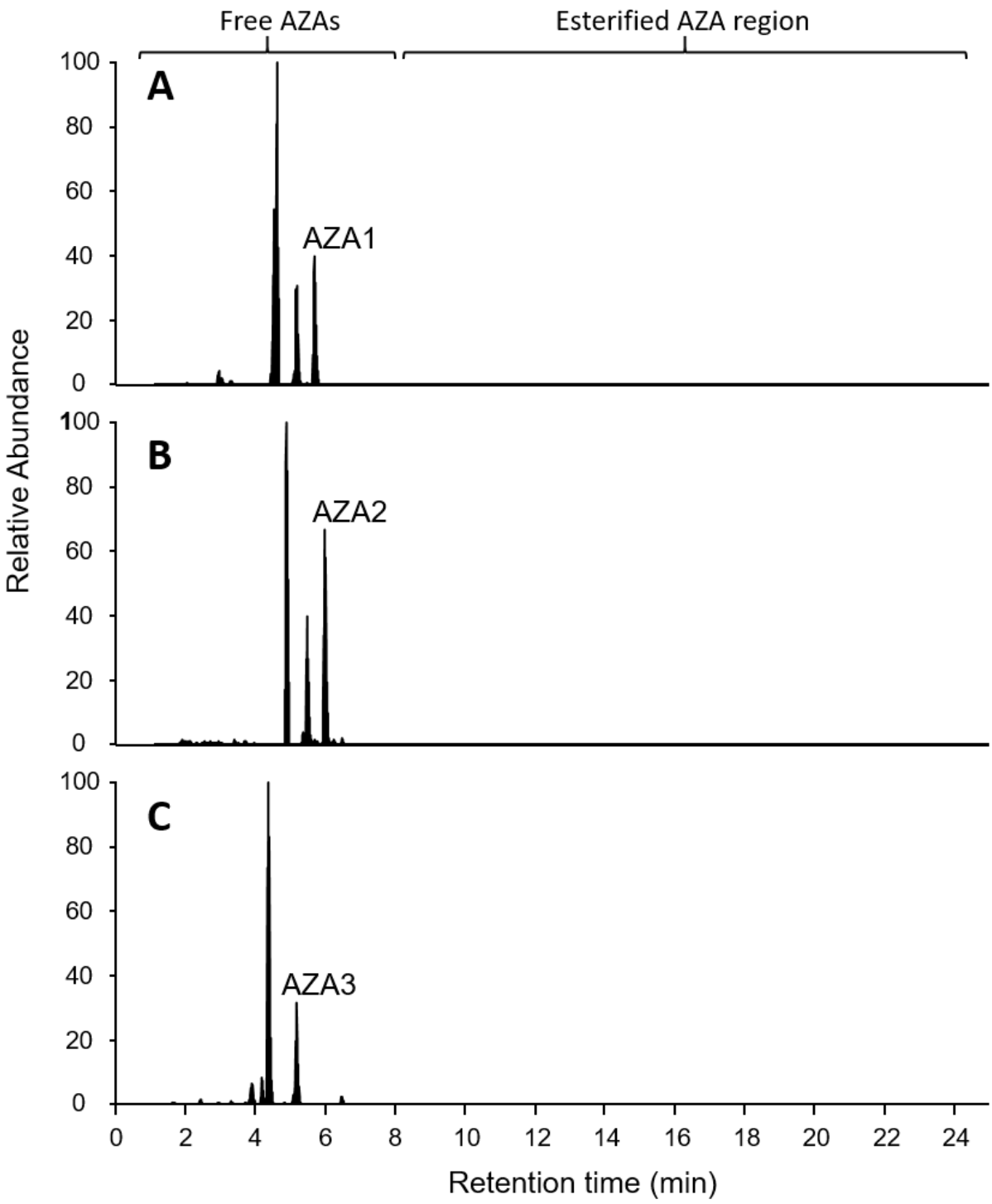

Figure S2. LC–HRMS/MS (method C) extracted diagnostic product ions at *m*/*z* 362.2690 and 168.1381 using a ±5 ppm mass tolerance from data-dependent acquisition to detect the presence of fatty acid esters of AZAs from the metabolism of: (A) AZA1; (B) AZA2, and; (C) AZA3.

In vitro metabolism of AZA1–3 in blue mussel hepatopancreatic fraction

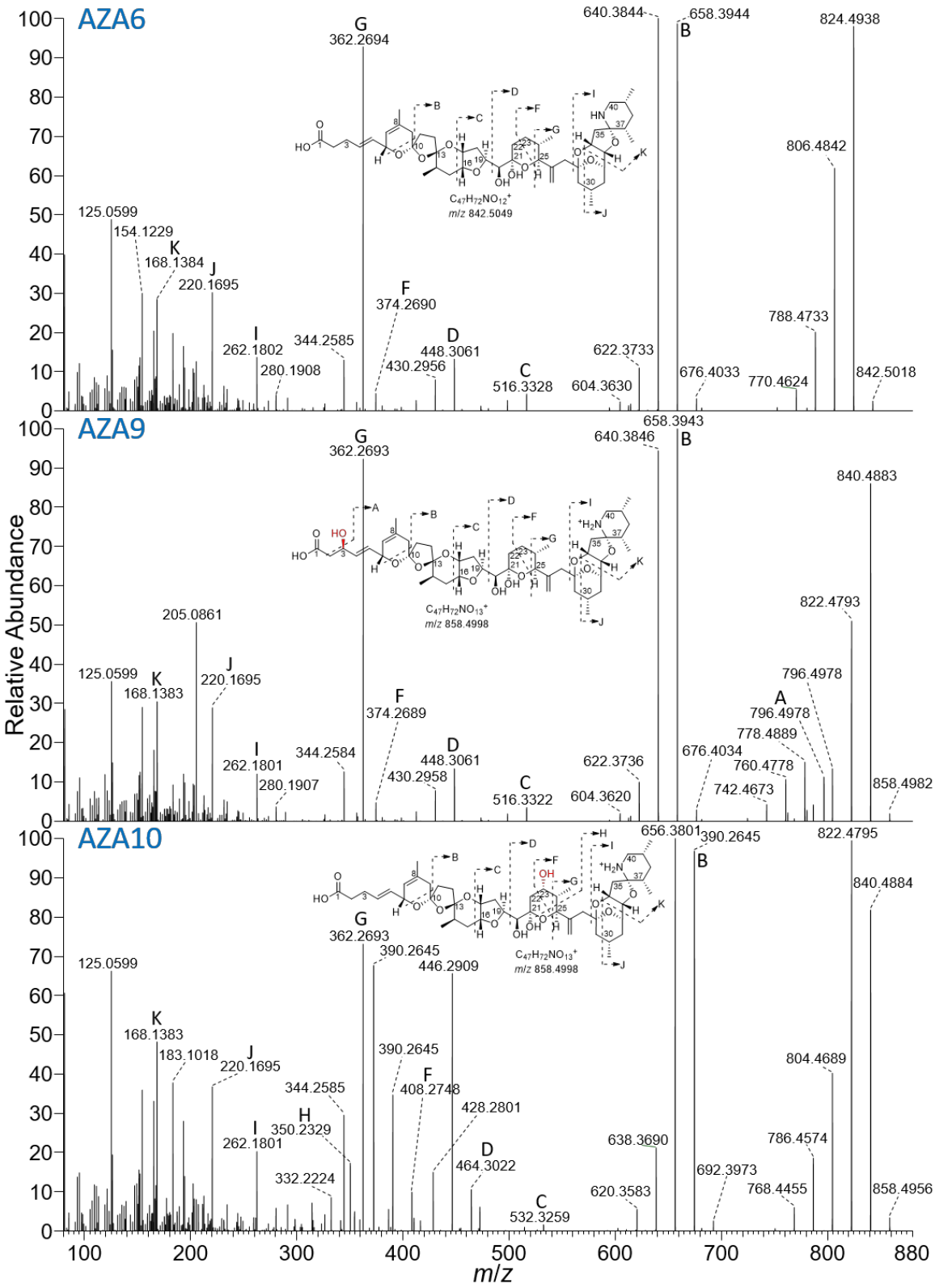

Figure S3. LC–HRMS/MS (method A) spectra of standards of: top, AZA6; middle, AZA9, and; AZA10. Major MS/MS fragments are marked with letters as denoted in Figure 3.

In vitro metabolism of AZA1–3 in blue mussel hepatopancreatic fraction

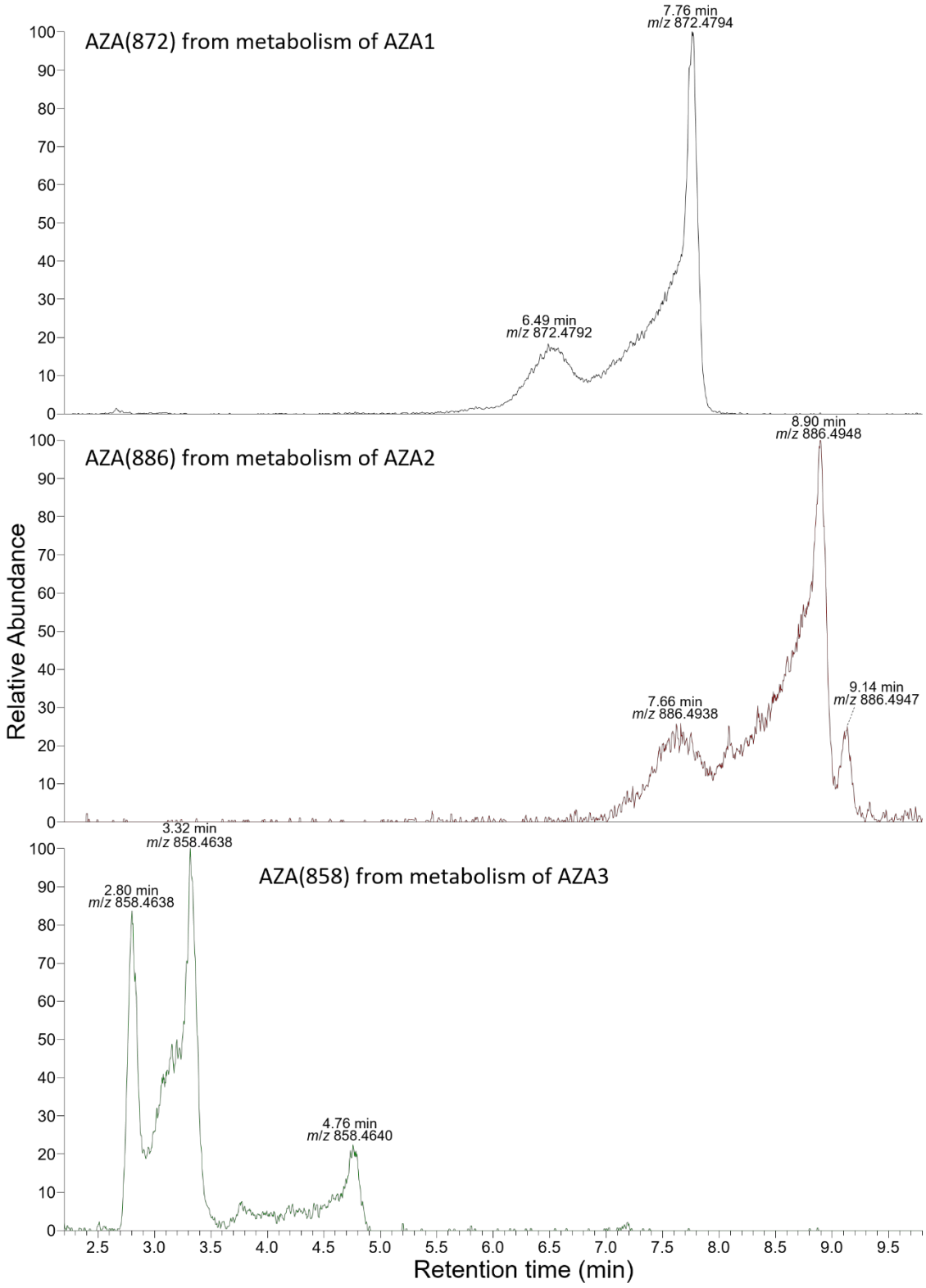

Figure S4. Full-scan LC–HRMS (method A) extracted ion (±5 ppm) chromatograms (2.2–9.8 min only) after 20 h metabolism, of: top, AZA1, at *m*/*z* 872.4791; middle, AZA2, at *m*/*z* 886.4947, and; AZA3, at *m*/*z* 858.4634.

In vitro metabolism of AZA1–3 in blue mussel hepatopancreatic fraction

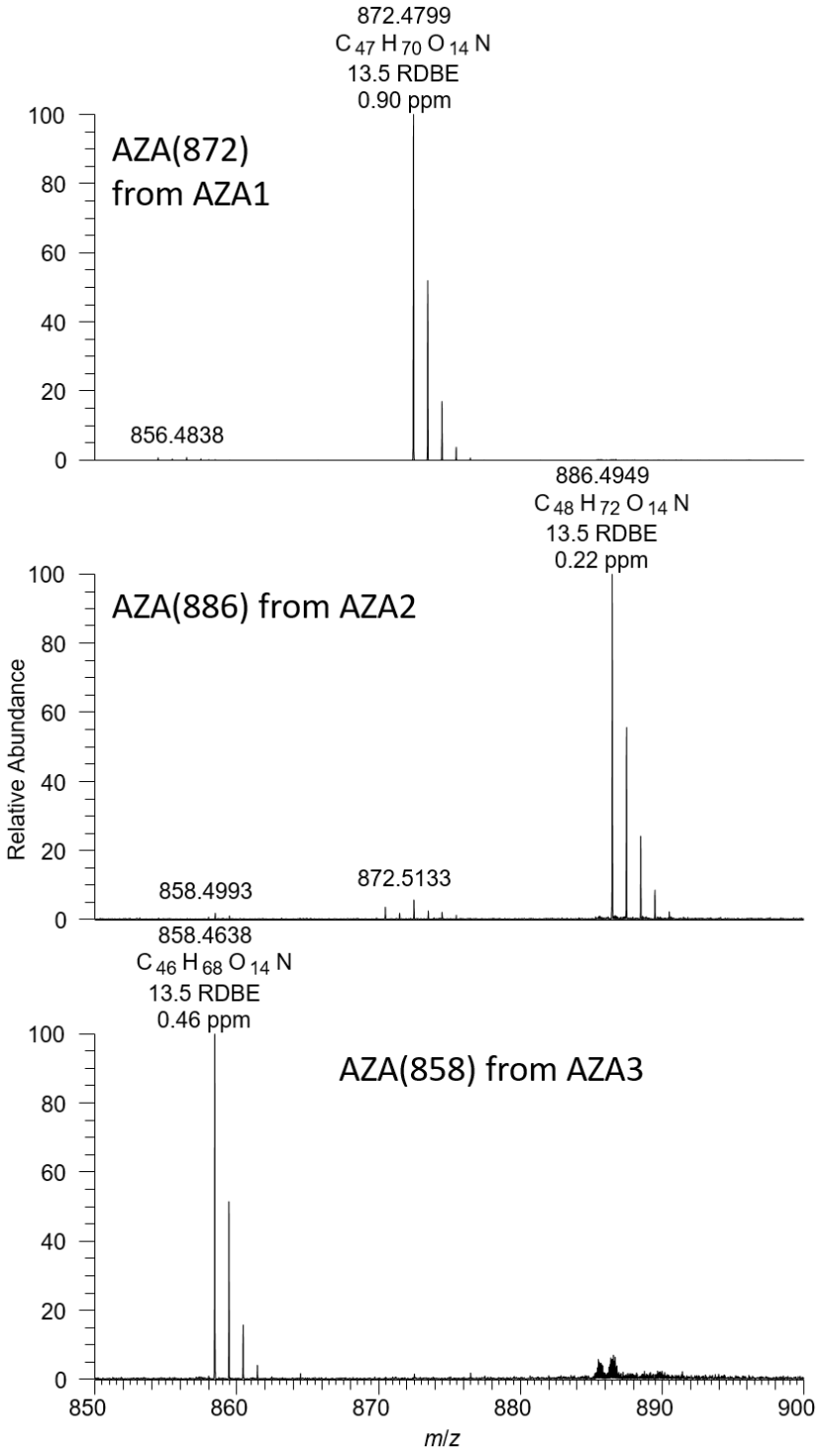

Figure S5. Full-scan LC–HRMS (method A) spectra of the broad peaks of AZA(872), AZA(886) and AZA(858) shown in the chromatograms in Figure S4. The $[M+H]^+$ ions are appended with the assigned formulae, number of rings plus double-bond equivalents (RDBE) and mass error (ppm) from the assigned formula, as reported by Xcalibur 4.0.

In vitro metabolism of AZA1–3 in blue mussel hepatopancreatic fraction

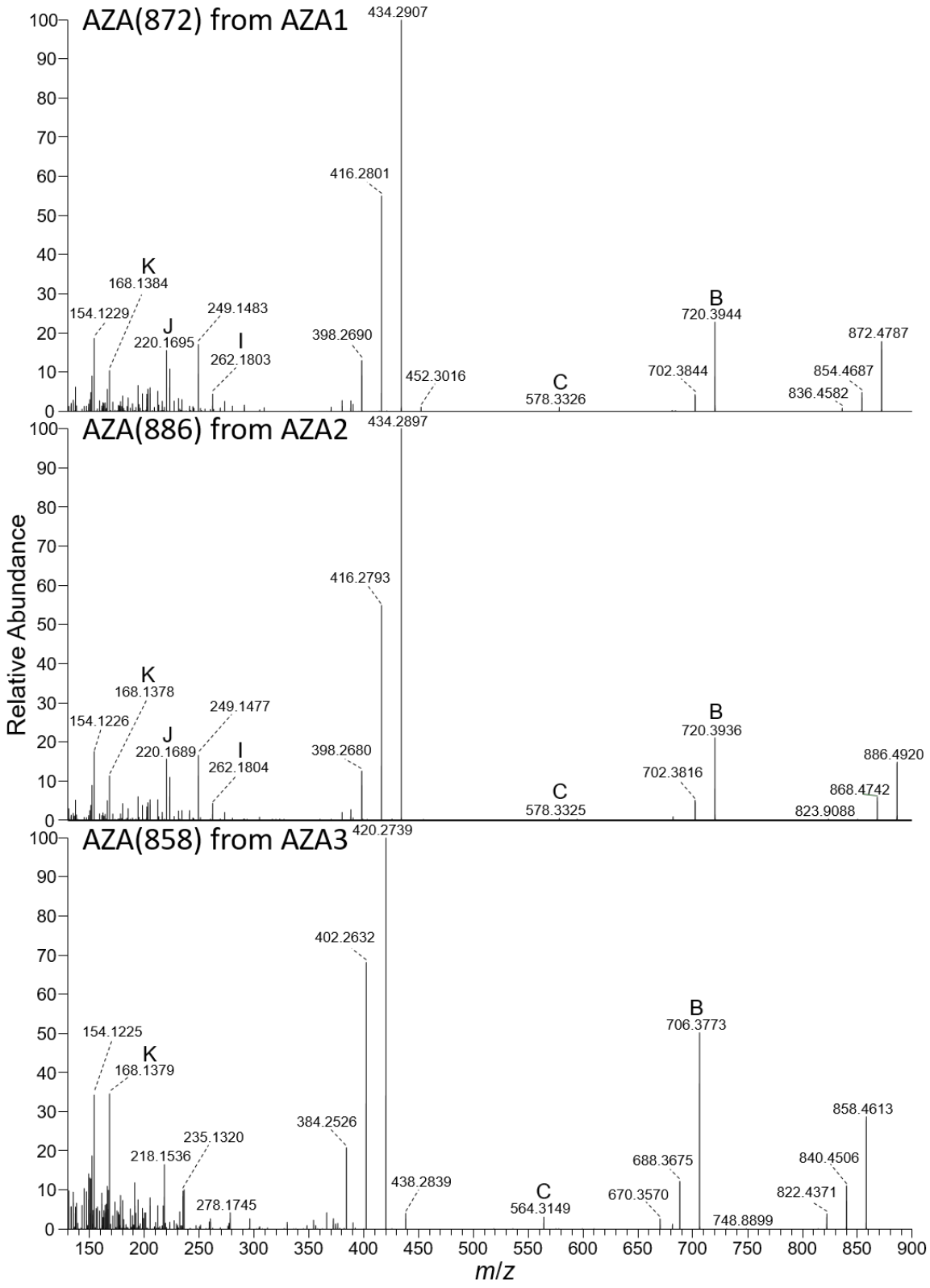

Figure S6. LC–HRMS/MS (method A) spectra of AZA(872), AZA(886) and AZA(858). Major identified MS/MS fragments are marked with letters on the structures as denoted in Figure 3.

In vitro metabolism of AZA1–3 in blue mussel hepatopancreatic fraction

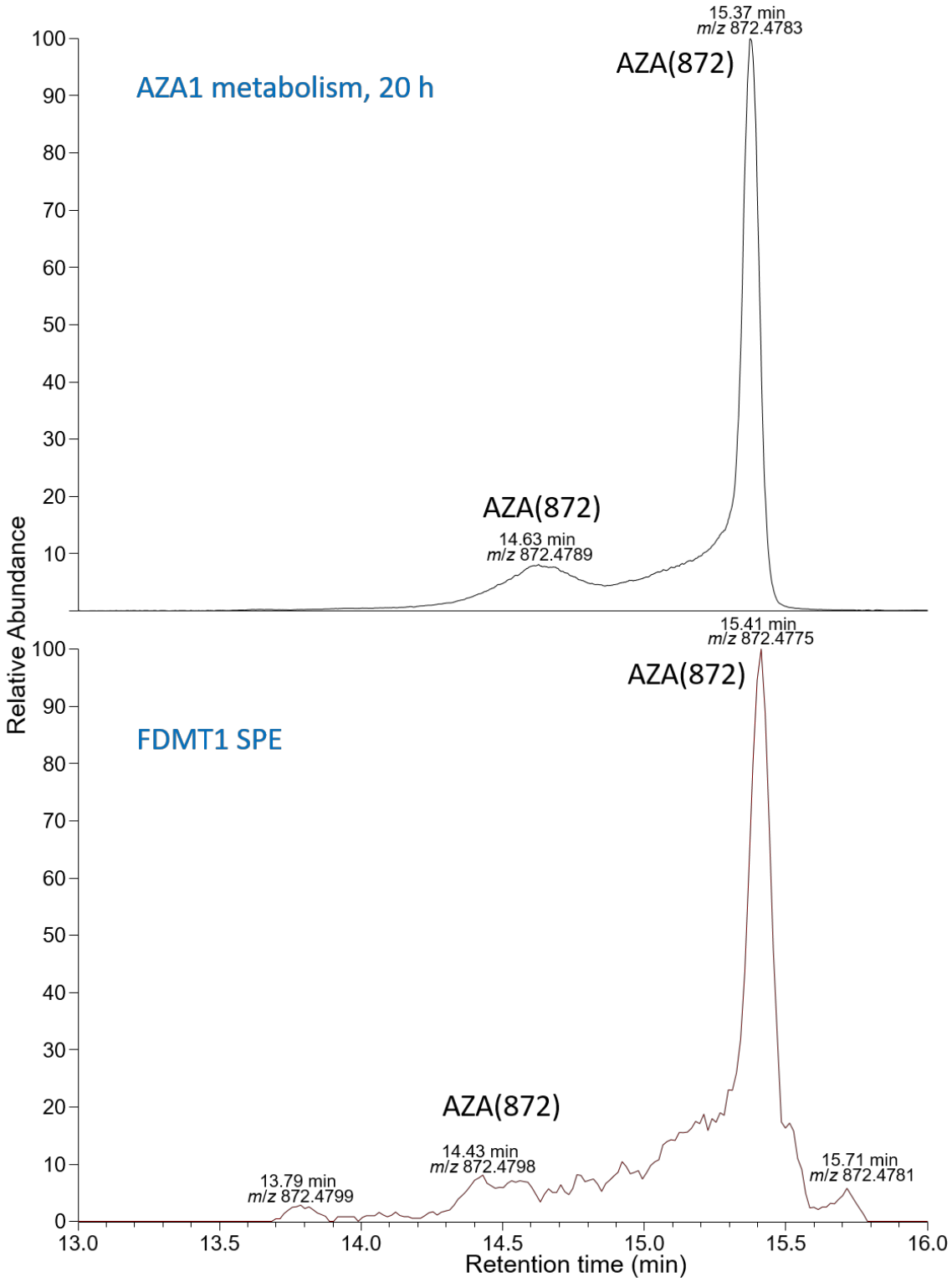

Figure S7. Extracted ion (*m/z* 872.4791 ±5 ppm) full-scan LC–HRMS (method B) chromatograms of: top, the AZA1 metabolism extract at 20 h, and; bottom, an SPE-concentrated extract of FDMT1 (Wright and McCarron, 2021). The early-eluting broad peaks are the partially characterized AZA(872).

In vitro metabolism of AZA1–3 in blue mussel hepatopancreatic fraction

Supplementary Information

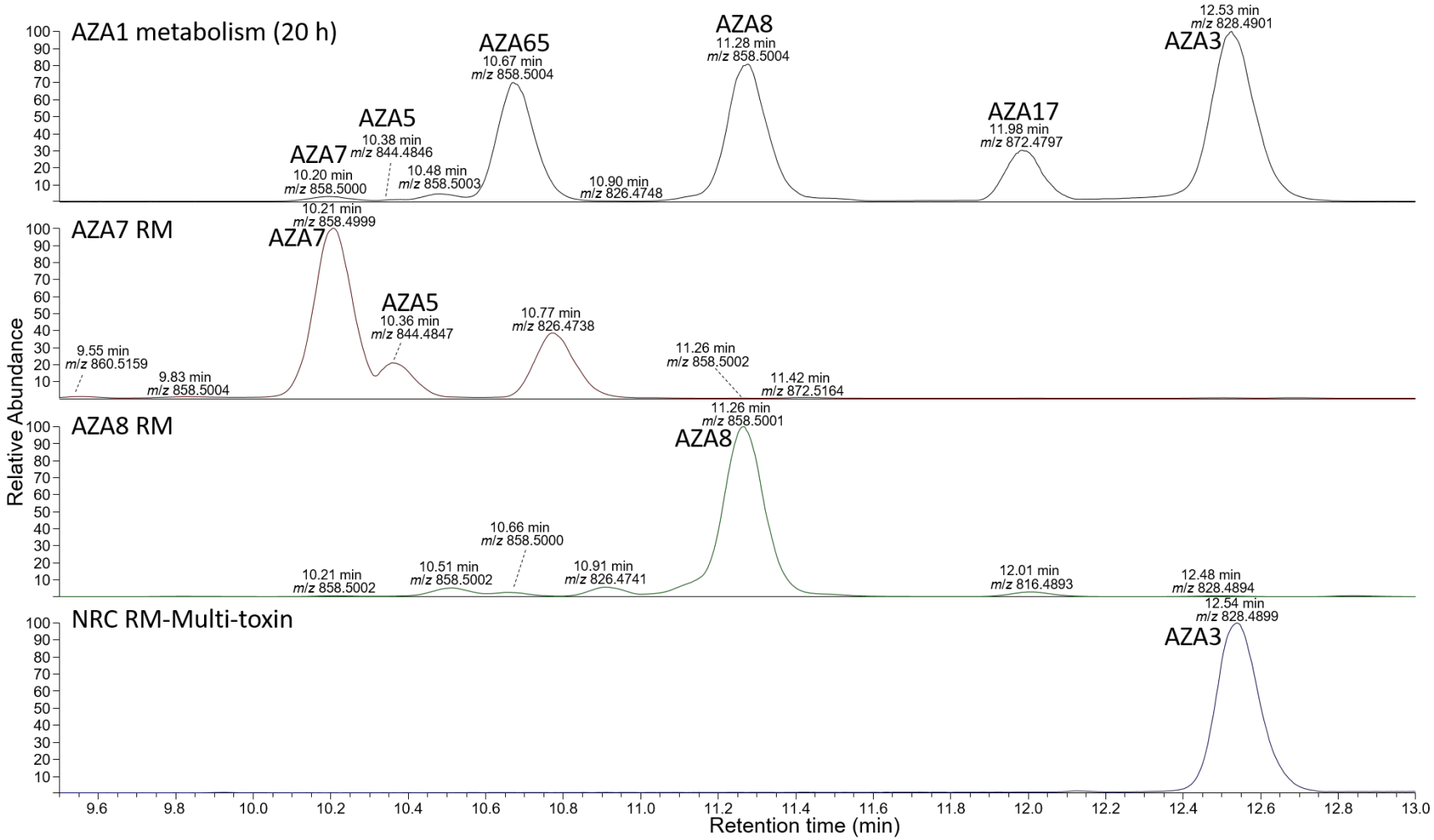

Figure S8. Full-scan LC–HRMS (method A) (*m*/*z* 800–900) chromatogram from: top, extract from metabolism of AZA1 for 20 h; middle panels, the standard of AZA7 containing AZA5 as a contaminant, and the standard of AZA8 (Kilcoyne et al., 2015), and; bottom, a mixed reference material containing AZA1, AZA2, and AZA3 (AZA1 and AZA2 elute later, see Figure S11).

In vitro metabolism of AZA1–3 in blue mussel hepatopancreatic fraction

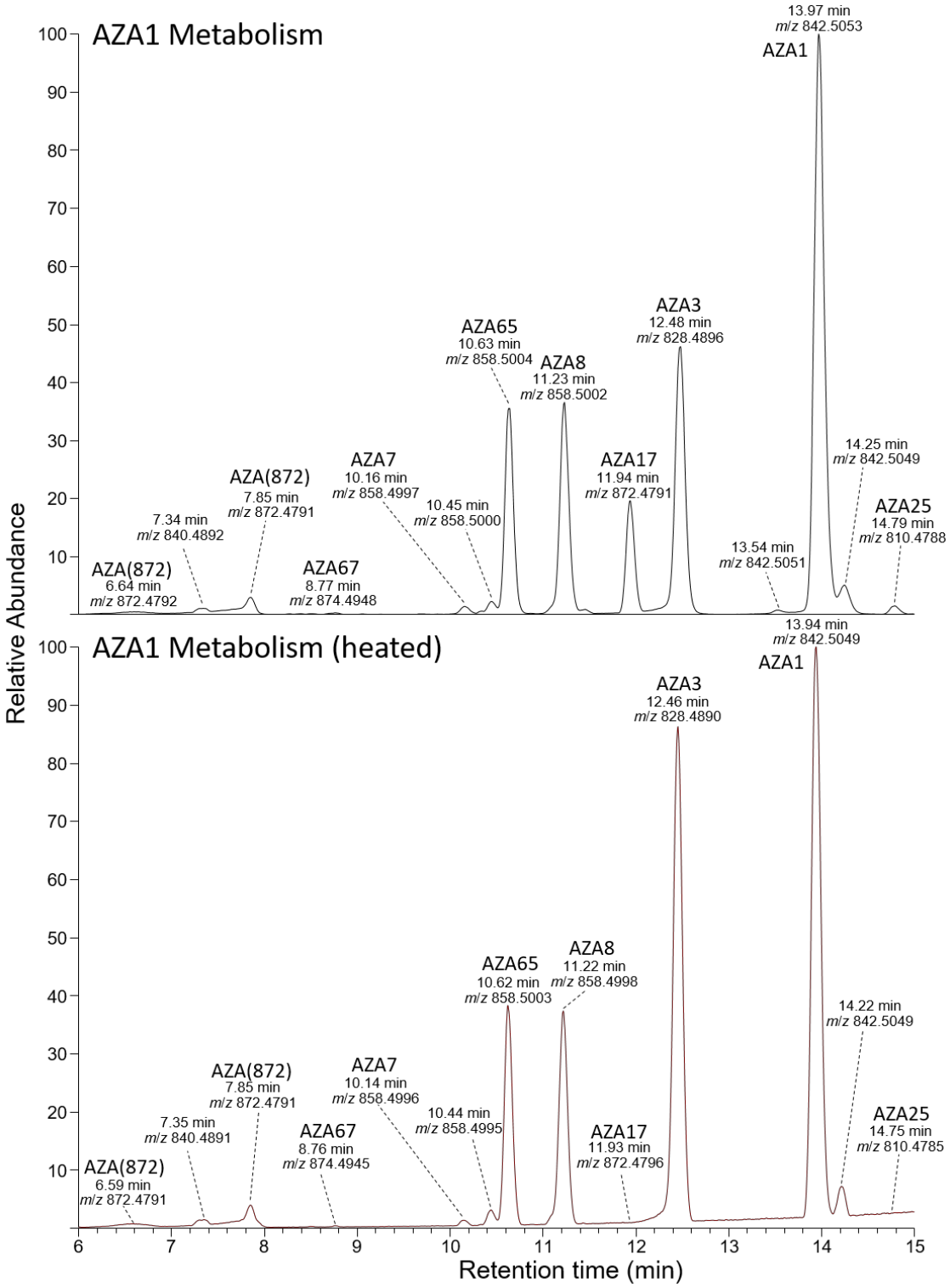

Figure S9. Full-scan LC–HRMS (method A) (*m*/*z* 800–900) showing the effect of heating an extract from metabolism (20 h) of AZA1 at 60 °C for 30 min. Note the almost complete disappearance of AZA17 and the increase in the intensity of the peak for AZA3, while the peaks of AZA1, AZA7, AZA8, AZA65, AZA67 and AZA(872) are essentially unaffected.

In vitro metabolism of AZA1–3 in blue mussel hepatopancreatic fraction

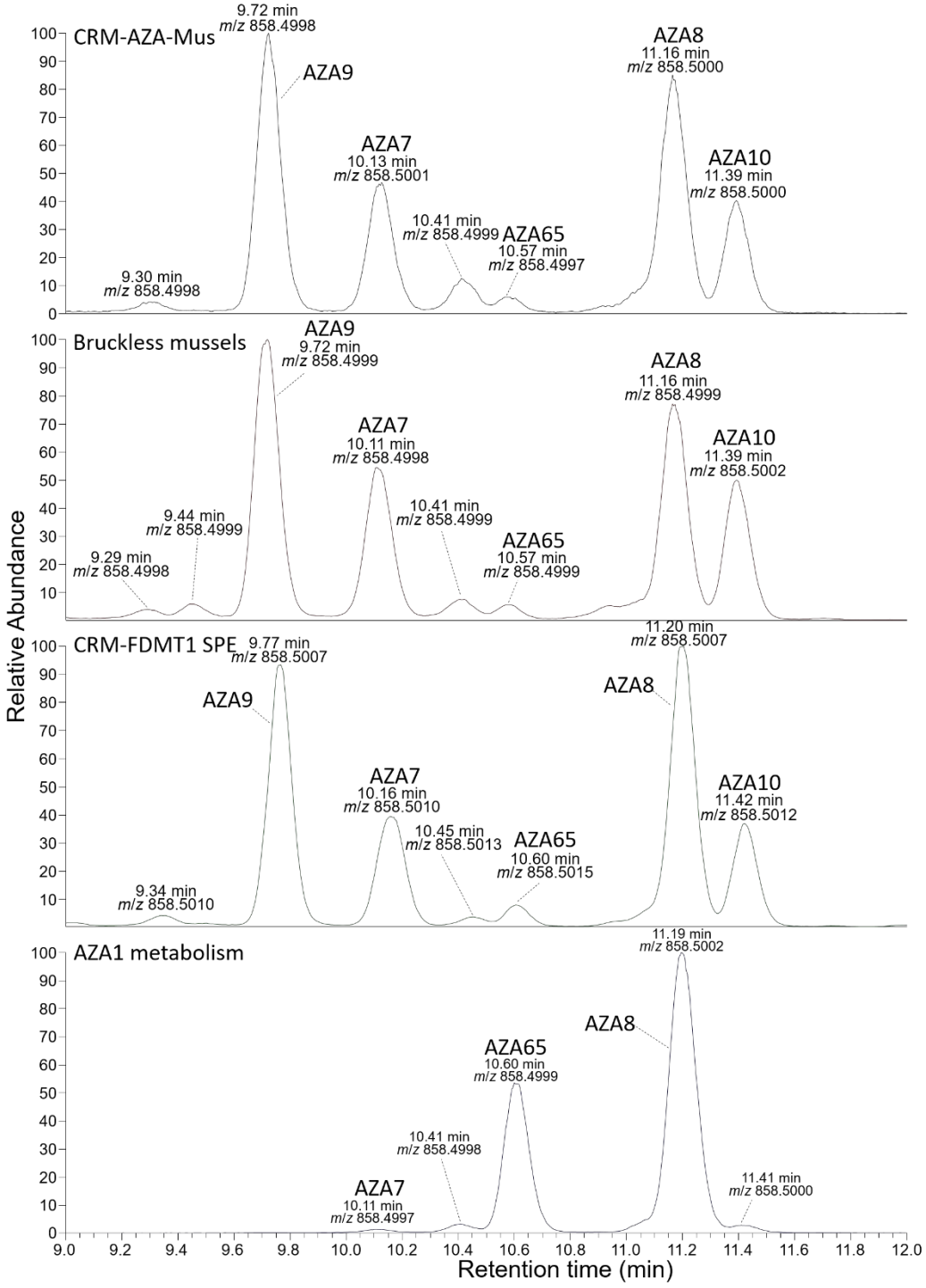

Figure S10. Extracted ion (*m*/*z* 858.4998 ±5 ppm) full-scan LC–HRMS (method A) chromatograms (9.0–12.0 min) of: top, an extract of NRC CRM-AZA-Mus (McCarron et al., 2015); an extract of mussels from Bruckless, Ireland; an SPE-concentrated extract of NRC CRM-FDMT1 (Wright and McCarron, 2021), and; bottom, the AZA1 metabolism extract at 20 h. This shows the presence of AZA65, whose identity was confirmed by analysis of its HRMS/MS spectra in the CRM-FDMT1 and AZA1 metabolism samples.

In vitro metabolism of AZA1–3 in blue mussel hepatopancreatic fraction

Supplementary Information

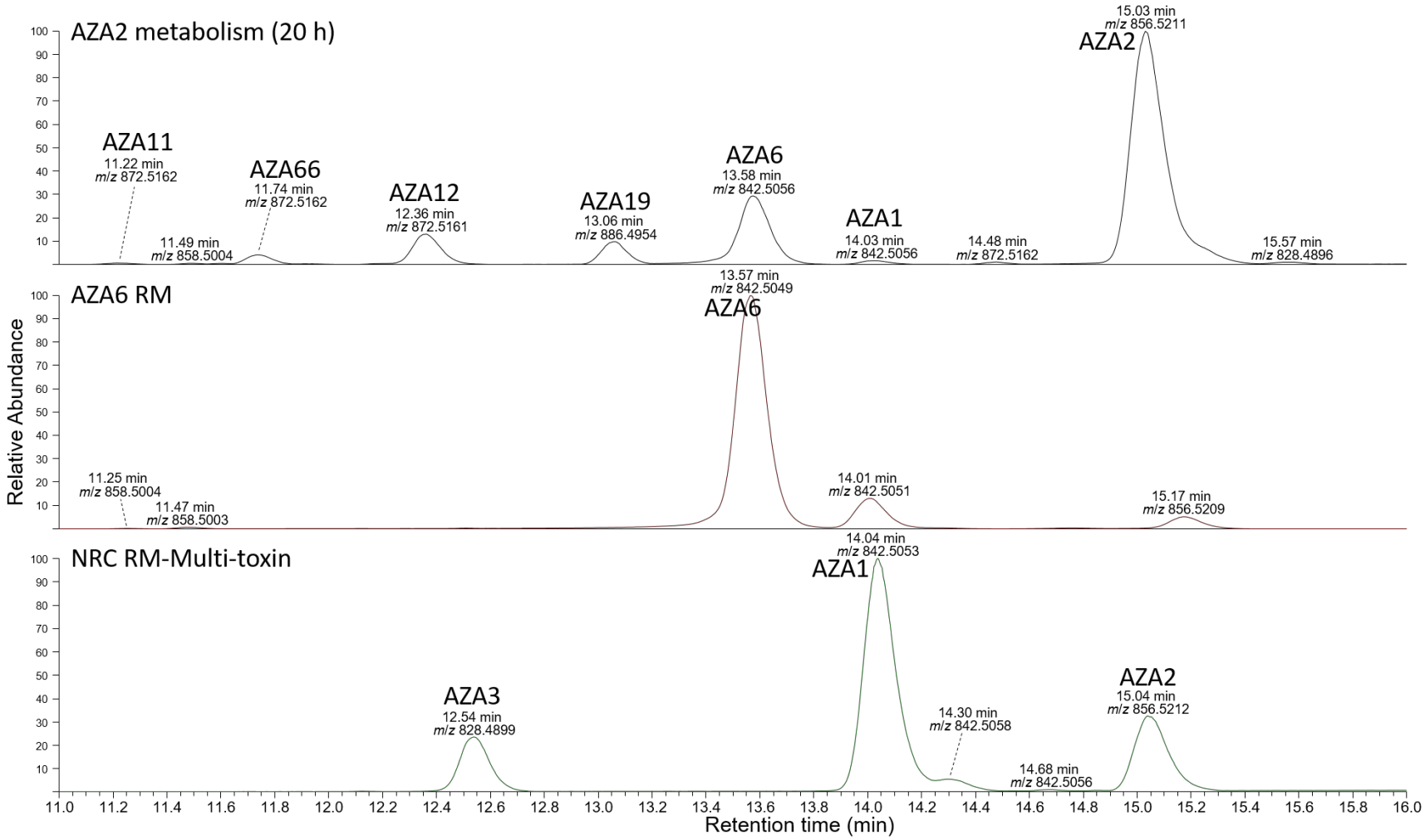

Figure S11. Full-scan LC–HRMS (method A) (*m*/*z* 800–900) chromatogram from: top, an extract from metabolism of AZA2 for 20 h; middle, the standard of AZA6 (Kilcoyne et al., 2015), and; bottom, a mixed reference material (RM-Multi-toxin) containing AZA1, AZA2 and AZA3.

In vitro metabolism of AZA1–3 in blue mussel hepatopancreatic fraction

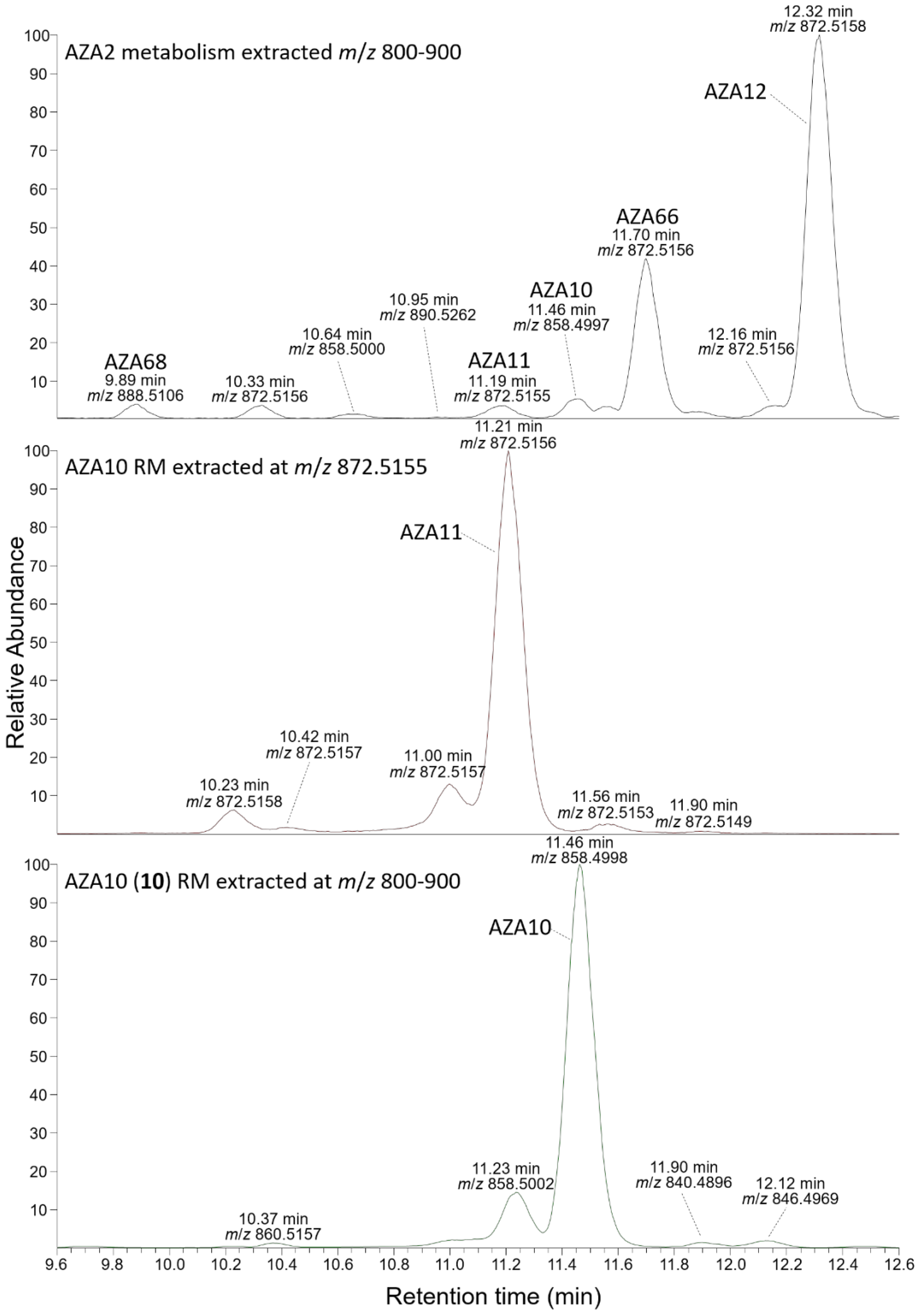

Figure S12. Full-scan LC–HRMS (method A) of: top, chromatogram (*m*/*z* 800–900) of an extract from metabolism of AZA2 for 20 h; middle, chromatogram of the standard of AZA10 contaminated by AZA11 (Kilcoyne et al., 2015) extracted at *m*/*z* 872.5155, and; bottom, chromatogram of the AZA 10 standard extracted at *m*/*z* 858.4998.

In vitro metabolism of AZA1–3 in blue mussel hepatopancreatic fraction

Supplementary Information

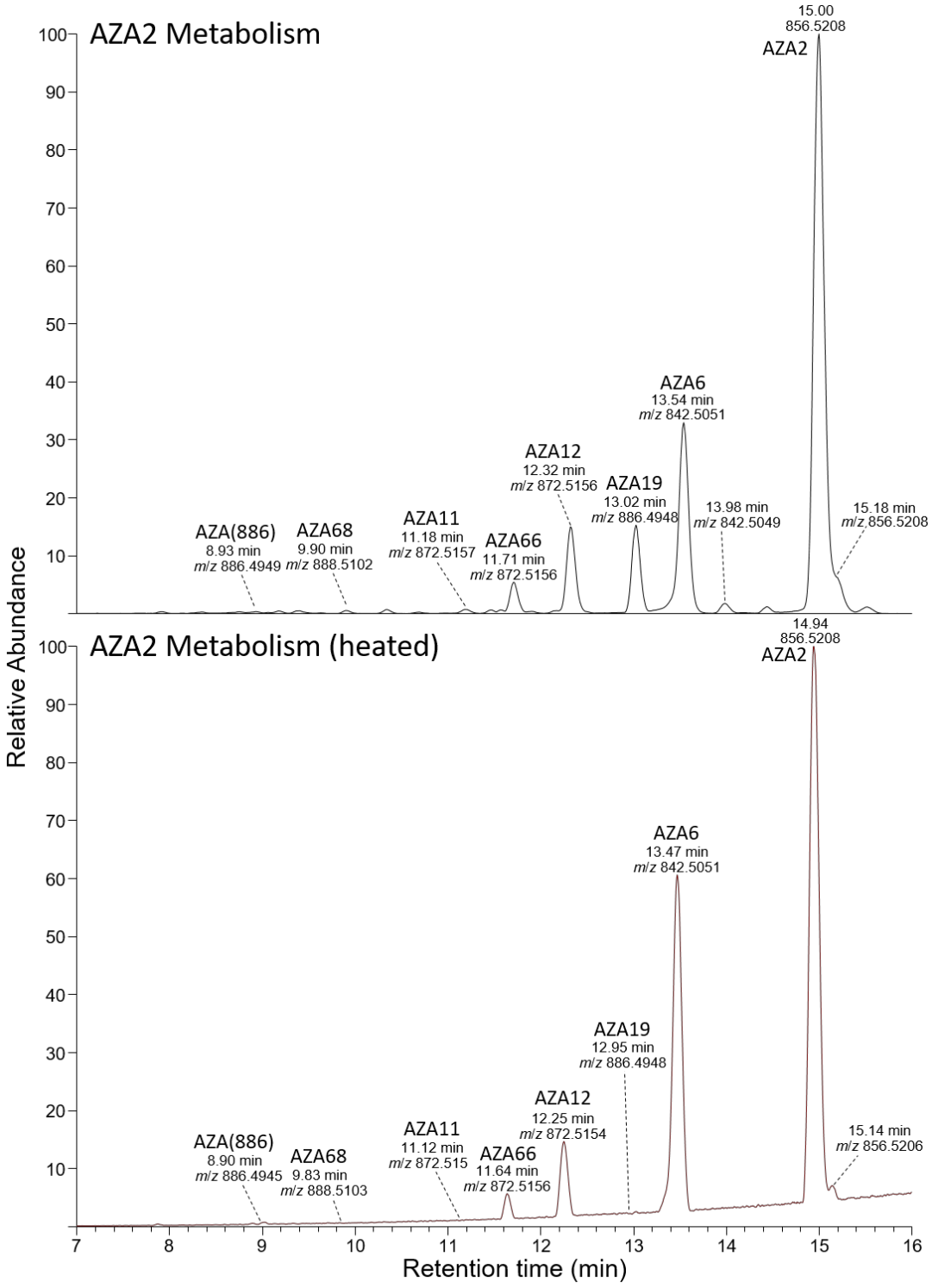

Figure S13. Full-scan LC–HRMS chromatogram (method A) (*m*/*z* 800–900) showing the effect of heating an extract from metabolism (20 h) of AZA2 (**2**) at 60 °C for 30 min. Note the almost complete disappearance of AZA19 and the increase in the intensity of the peak for AZA6, while the peaks of AZA2, AZA11, AZA12, AZA66, AZA68 and AZA(886) are essentially unaffected.

In vitro metabolism of AZA1–3 in blue mussel hepatopancreatic fraction

Supplementary Information

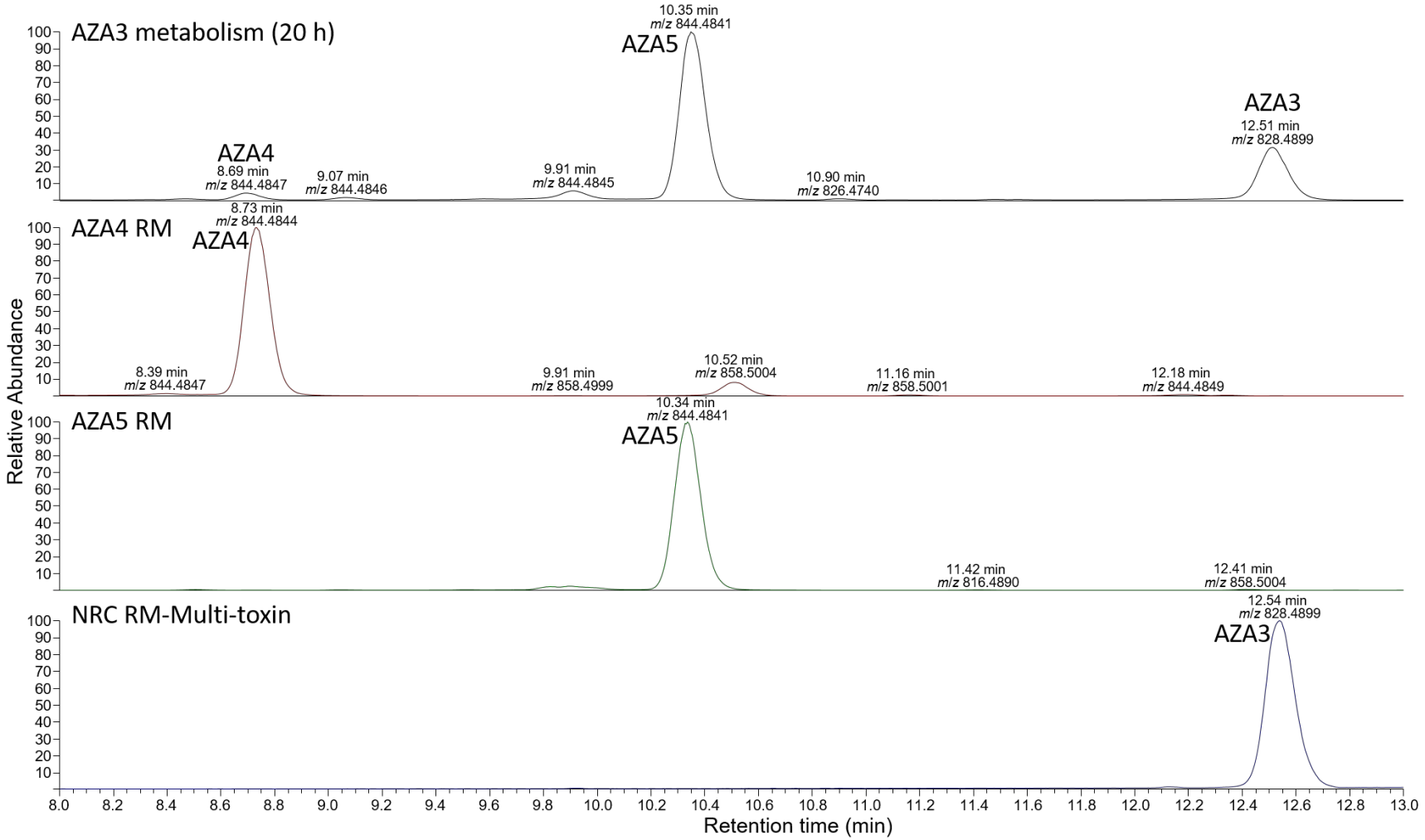

Figure S14. Full-scan LC–HRMS (method A) (*m*/*z* 800–900) chromatogram from: top, extract from metabolism of AZA3 for 20 h; middle panels, the standards of AZA4, and of AZA5 (Kilcoyne et al., 2015), and; bottom, a mixed reference material containing AZA1, AZA2, and AZA3 (AZA1 and AZA2 elute later, see Figure S11).

In vitro metabolism of AZA1–3 in blue mussel hepatopancreatic fraction

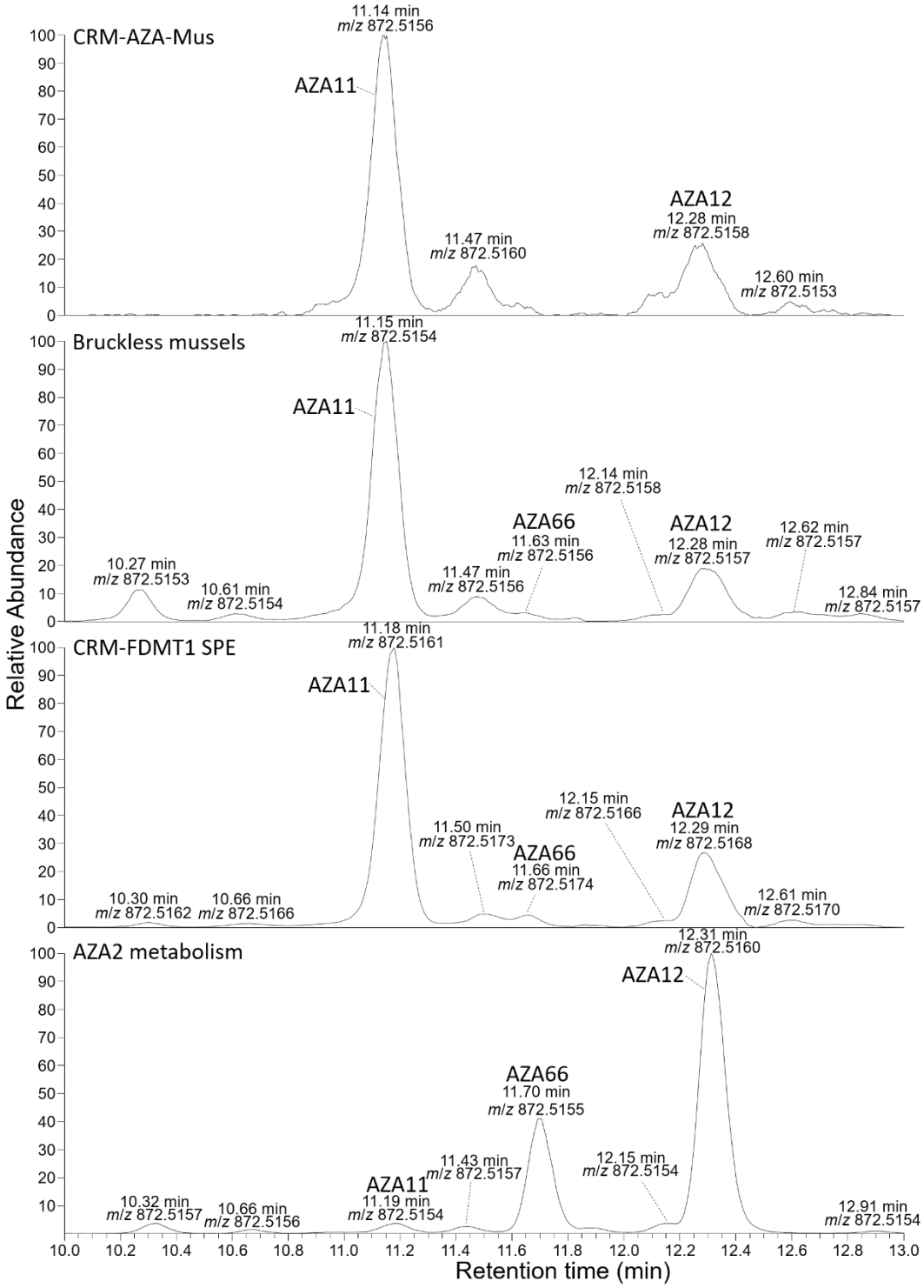

Figure S15. Extracted ion (*m*/*z* 872.5155 ±5 ppm) full-scan LC–HRMS (method A) chromatograms (10.0–13.0 min) of: top, an extract of NRC CRM-AZA-Mus (McCarron et al., 2015); an extract of mussels from Bruckless, Ireland; an SPE-concentrated extract of NRC CRM-FDMT1 (Wright and McCarron, 2021), and; bottom, the AZA2 metabolism extract at 20 h. This shows the presence of AZA66, whose identity was confirmed from analysis its HRMS/MS spectra in the CRM-FDMT1 and AZA2 metabolism samples.

In vitro metabolism of AZA1–3 in blue mussel hepatopancreatic fraction

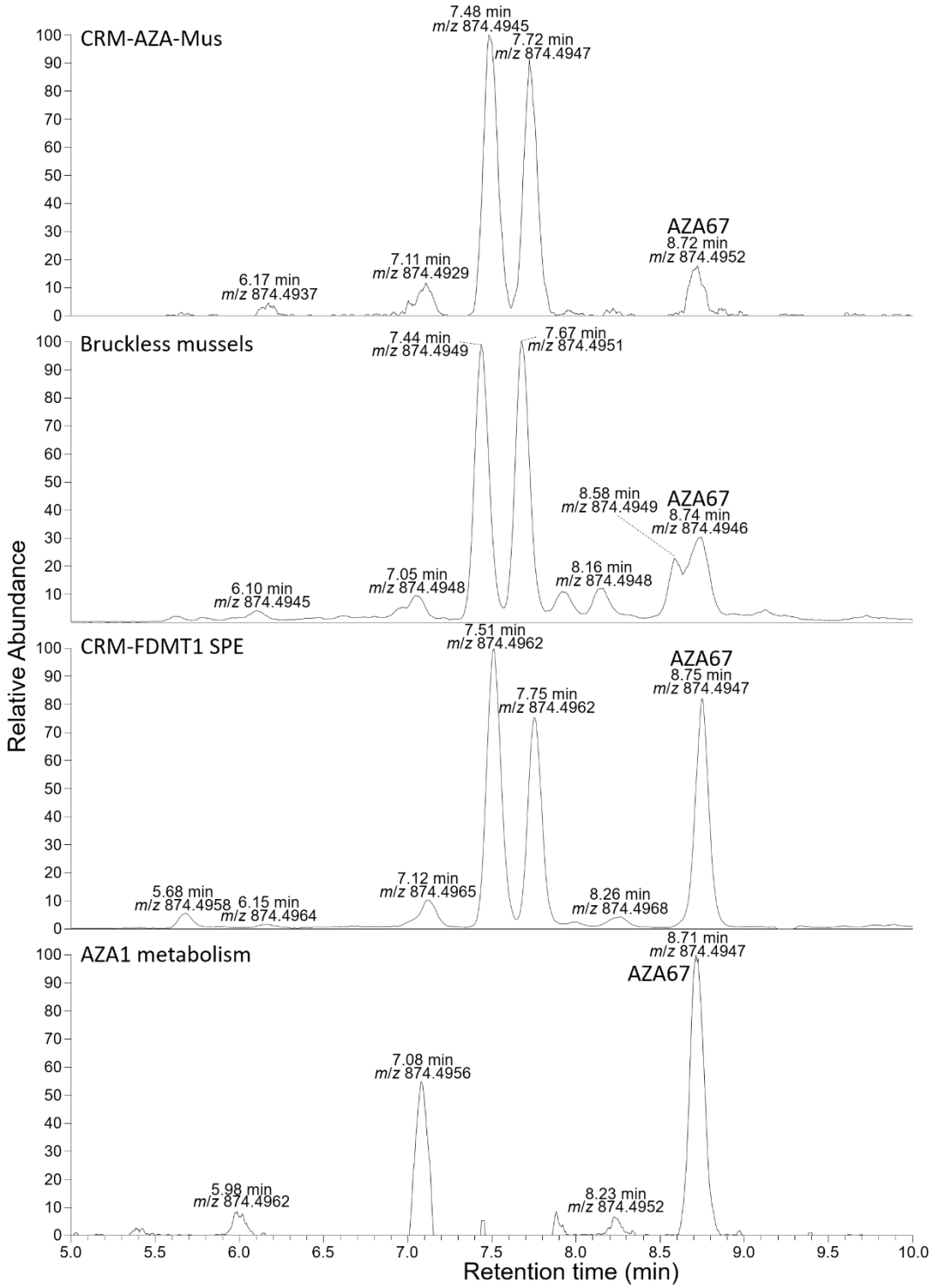

Figure S16. Extracted ion (*m*/*z* 874.4947 ±5 ppm) full-scan LC–HRMS (method A) chromatograms (5.0–10.0 min) of: top, an extract of NRC CRM-AZA-Mus (McCarron et al., 2015); an extract of mussels from Bruckless, Ireland; an SPE-concentrated extract of NRC CRM-FDMT1 (Wright and McCarron, 2021), and; bottom, the AZA1 metabolism extract at 20 h. This shows the presence of AZA67, whose identity was confirmed from analysis its HRMS/MS spectra in the CRM-FDMT1 and AZA1 metabolism samples.

In vitro metabolism of AZA1–3 in blue mussel hepatopancreatic fraction

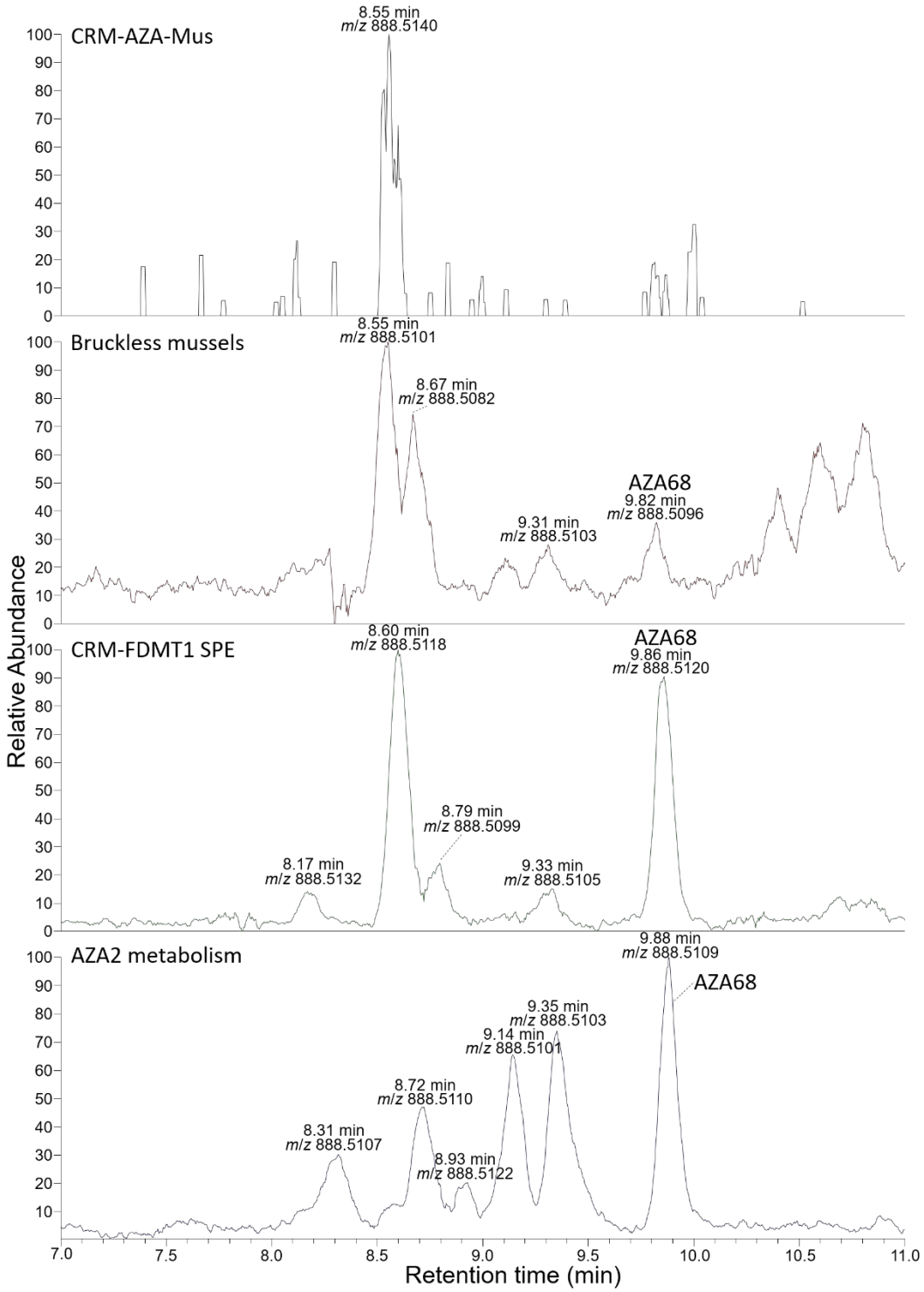

Figure S17. Extracted ion (*m*/*z* 888.5104 ±5 ppm) full-scan LC–HRMS (method A) chromatograms (7.0–11.0 min) of: top, NRC CRM-AZA-Mus (McCarron et al., 2015); an extract of mussels from Bruckless, Ireland; an SPE-concentrated extract of NRC CRM-FDMT1 (Wright and McCarron, 2021), and; bottom, the AZA2 metabolism extract at 20 h. This shows the presence of AZA68, whose identity was confirmed from analysis its HRMS/MS spectra in the CRM-FDMT1 and AZA2 metabolism samples.

In vitro metabolism of AZA1–3 in blue mussel hepatopancreatic fraction

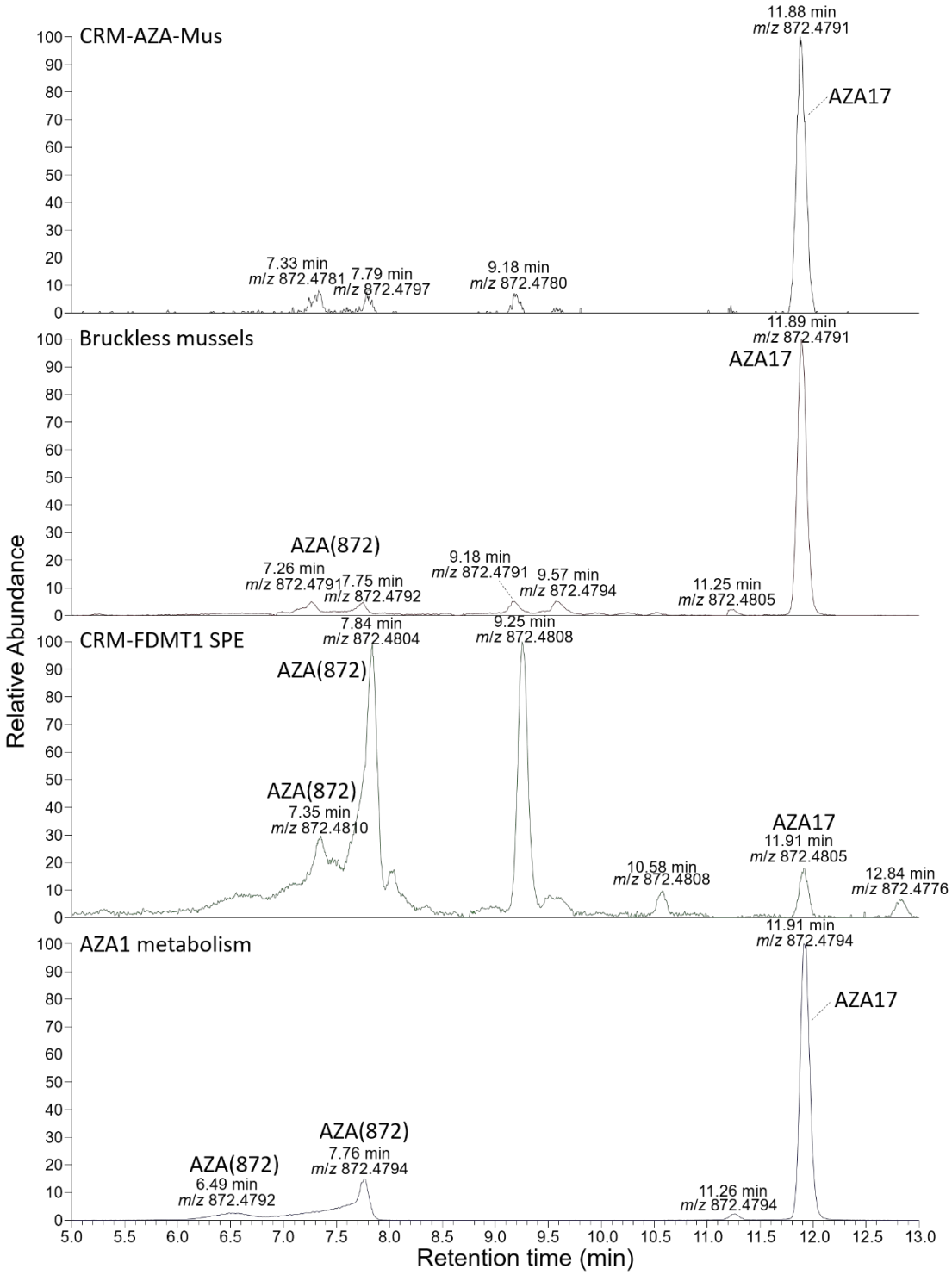

Figure S18. Extracted ion (*m*/*z* 872.4791 ±5 ppm) full-scan LC–HRMS (method A) chromatograms (5.0–13.0 min) of: top, an extract of NRC CRM-AZA-Mus (McCarron et al., 2015); an extract of mussels from Bruckless, Ireland; an SPE-concentrated extract of NRC CRM-FDMT1 (Wright and McCarron, 2021), and; bottom, the AZA1 metabolism extract at 20 h. This shows the presence of AZA17 and AZA(872) in the CRM-FDMT1 and AZA1 metabolism samples.

In vitro metabolism of AZA1–3 in blue mussel hepatopancreatic fraction

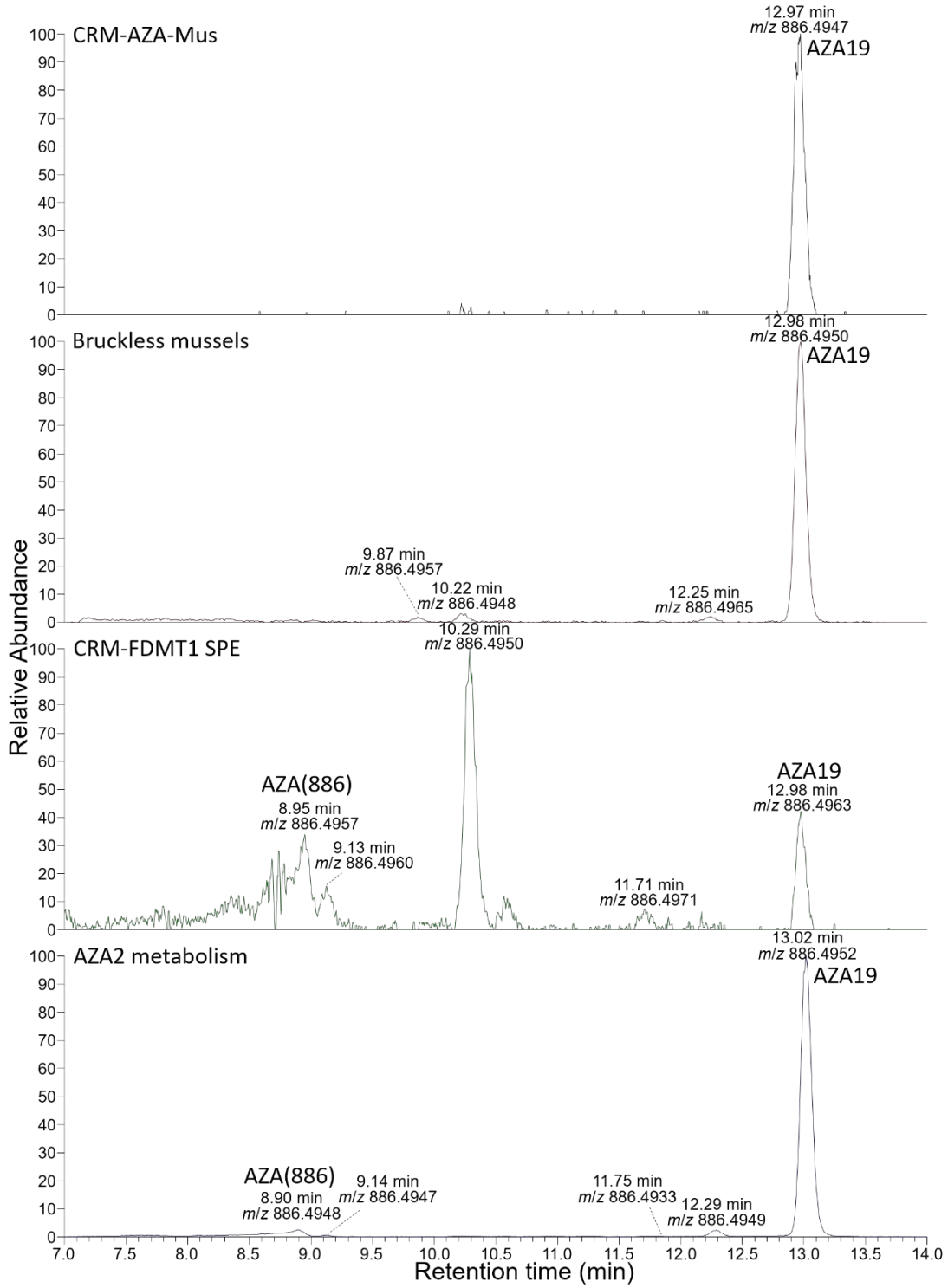

Figure S19. Extracted ion (*m*/*z* 886.4947 ±5 ppm) full-scan LC–HRMS (method A) chromatograms (7.0–14.0 min) of: top, an extract of NRC CRM-AZA-Mus (McCarron et al., 2015); an extract of mussels from Bruckless, Ireland; an SPE-concentrated extract of NRC CRM-FDMT1 (Wright and McCarron, 2021), and; bottom, the AZA2 metabolism extract at 20 h. This shows the presence of AZA19 and AZA(886) in the CRM-FDMT1 and AZA2 metabolism samples.

In vitro metabolism of AZA1–3 in blue mussel hepatopancreatic fraction

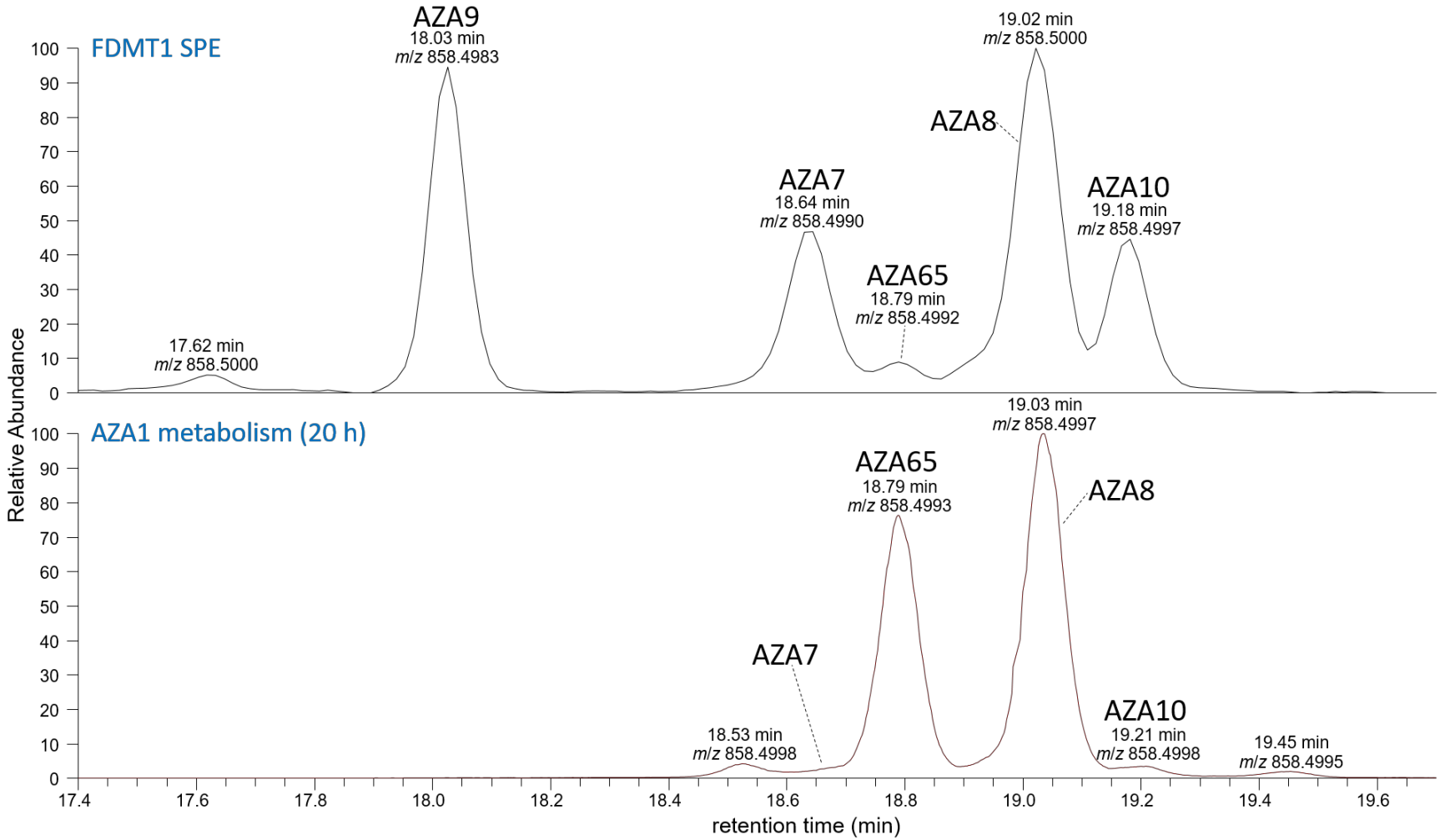

Figure S20. Extracted ion (*m/z* 858.4998 ±5 ppm) full-scan LC–HRMS (method B) chromatograms (17.4–19.7 min) of: top, an SPE-concentrated extract of NRC CRM-FDMT1 (Wright and McCarron, 2021), and; bottom, the AZA1 metabolism extract at 20 h. This confirms the presence of AZA65 in both the CRM-FDMT1 and AZA1 metabolism samples. The peak for AZA65 in FDMT1 SPE concentrate also displayed an appropriate HRMS/MS spectrum.

In vitro metabolism of AZA1–3 in blue mussel hepatopancreatic fraction

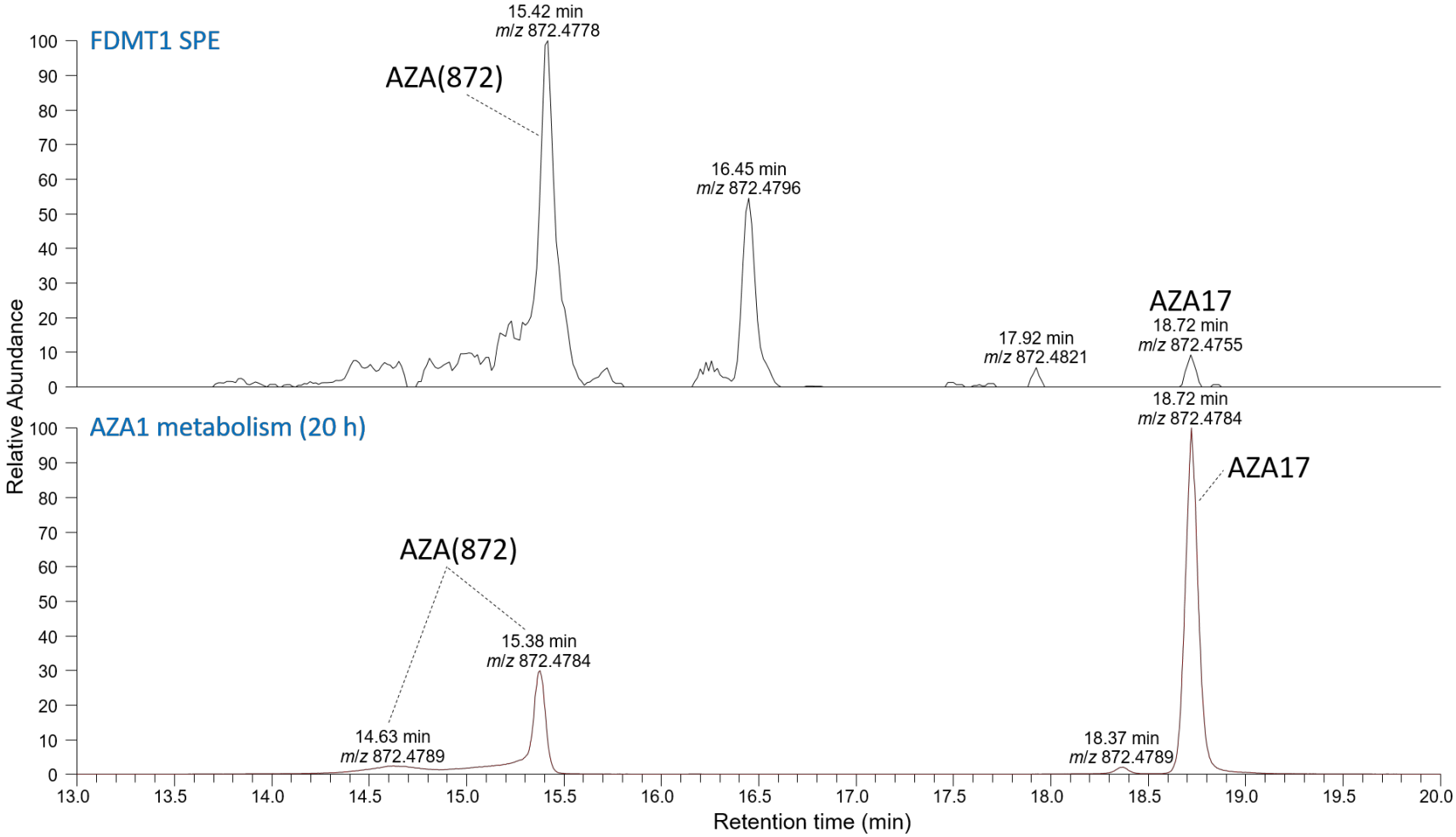

Figure S21. Extracted ion (*m/z* 872.4791 ±5 ppm) full-scan LC–HRMS (method B) chromatograms (13–20 min) of: top, an SPE-concentrated extract of NRC CRM-FDMT1 (Wright and McCarron, 2021), and; bottom, the AZA1 metabolism extract at 20 h. This confirms the presence of AZA(872) and AZA17 in both the CRM-FDMT1 and AZA1 metabolism samples.

In vitro metabolism of AZA1–3 in blue mussel hepatopancreatic fraction

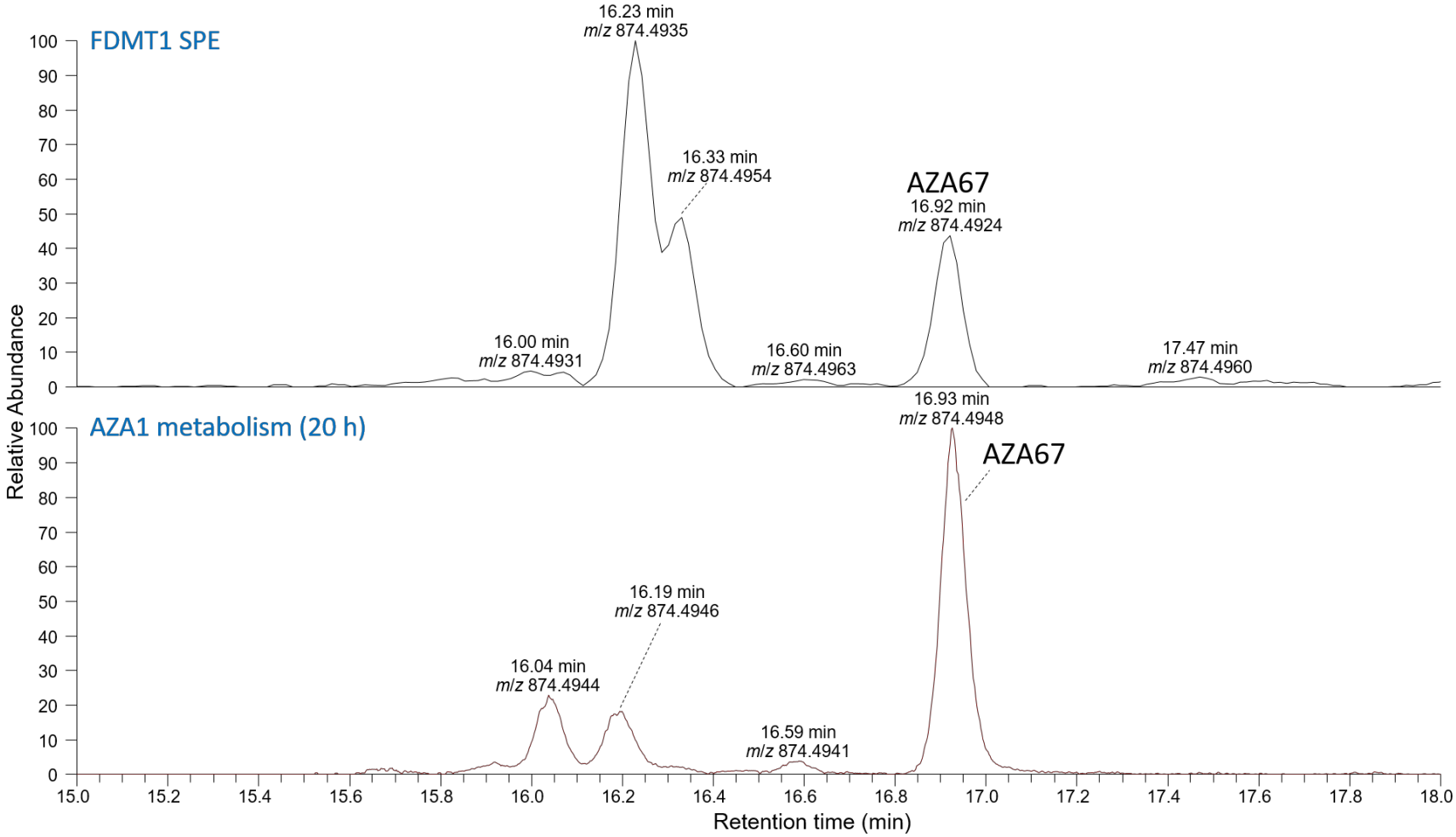

Figure S22. Extracted ion (*m*/*z* 874.4947 ±5 ppm) full-scan LC–HRMS (method B) chromatograms (15–18 min) of: top, an SPE-concentrated extract of NRC CRM-FDMT1 (Wright and McCarron, 2021), and; bottom, the AZA1 metabolism extract at 20 h. This confirms the presence of AZA67 in both the CRM-FDMT1 and AZA1 metabolism samples. The peak for AZA67 in FDMT1 SPE concentrate also displayed an appropriate HRMS/MS spectrum.

In vitro metabolism of AZA1–3 in blue mussel hepatopancreatic fraction

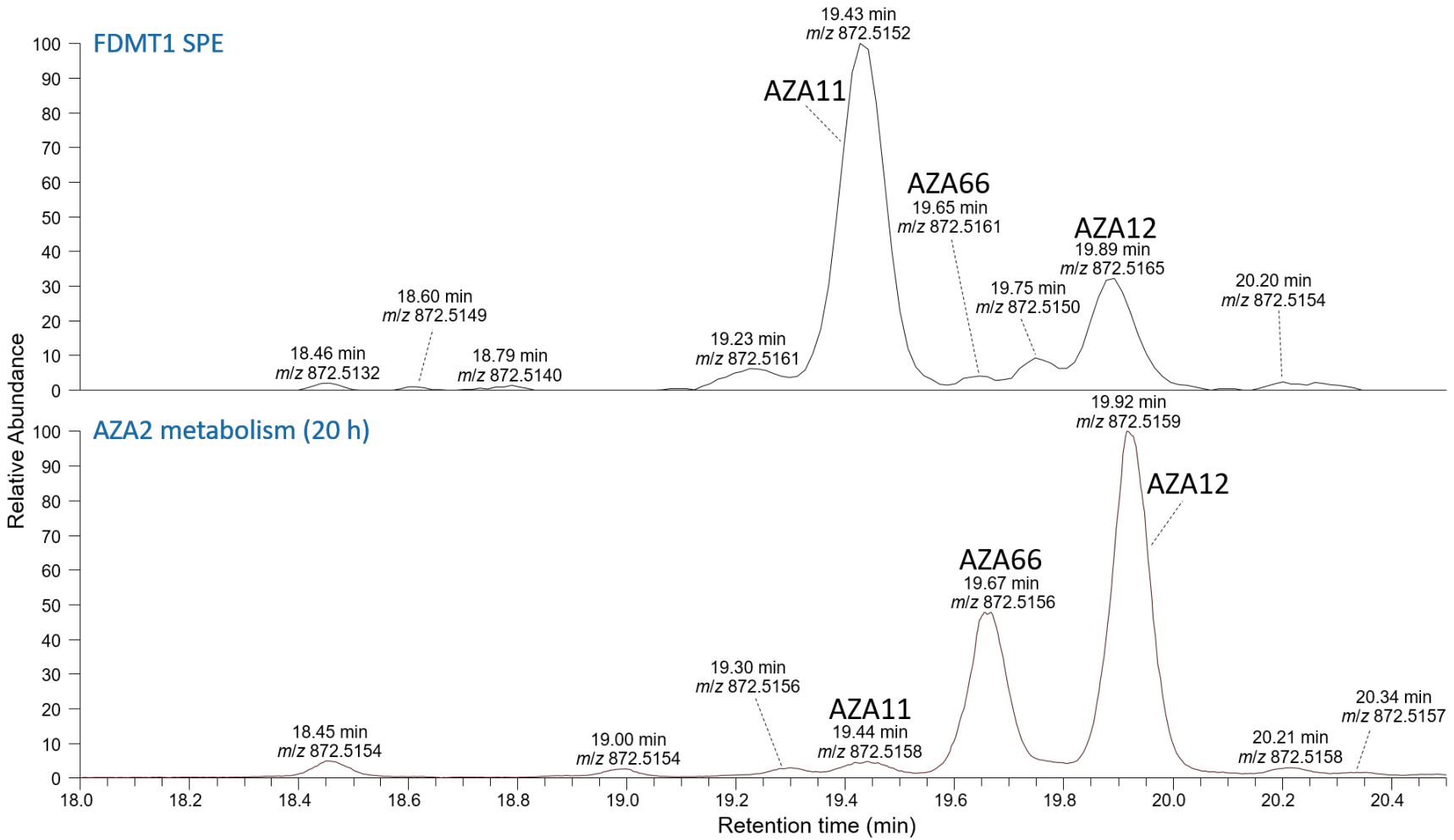

Figure S23. Extracted ion (*m/z* 872.5155 ±5 ppm) full-scan LC–HRMS (method B) chromatograms (18–20.5 min) of: top, an SPE-concentrated extract of NRC CRM-FDMT1 (Wright and McCarron, 2021), and; bottom, the AZA2 metabolism extract at 20 h. This confirms the presence of AZA66 in both the CRM-FDMT1 and AZA2 metabolism samples.

In vitro metabolism of AZA1–3 in blue mussel hepatopancreatic fraction

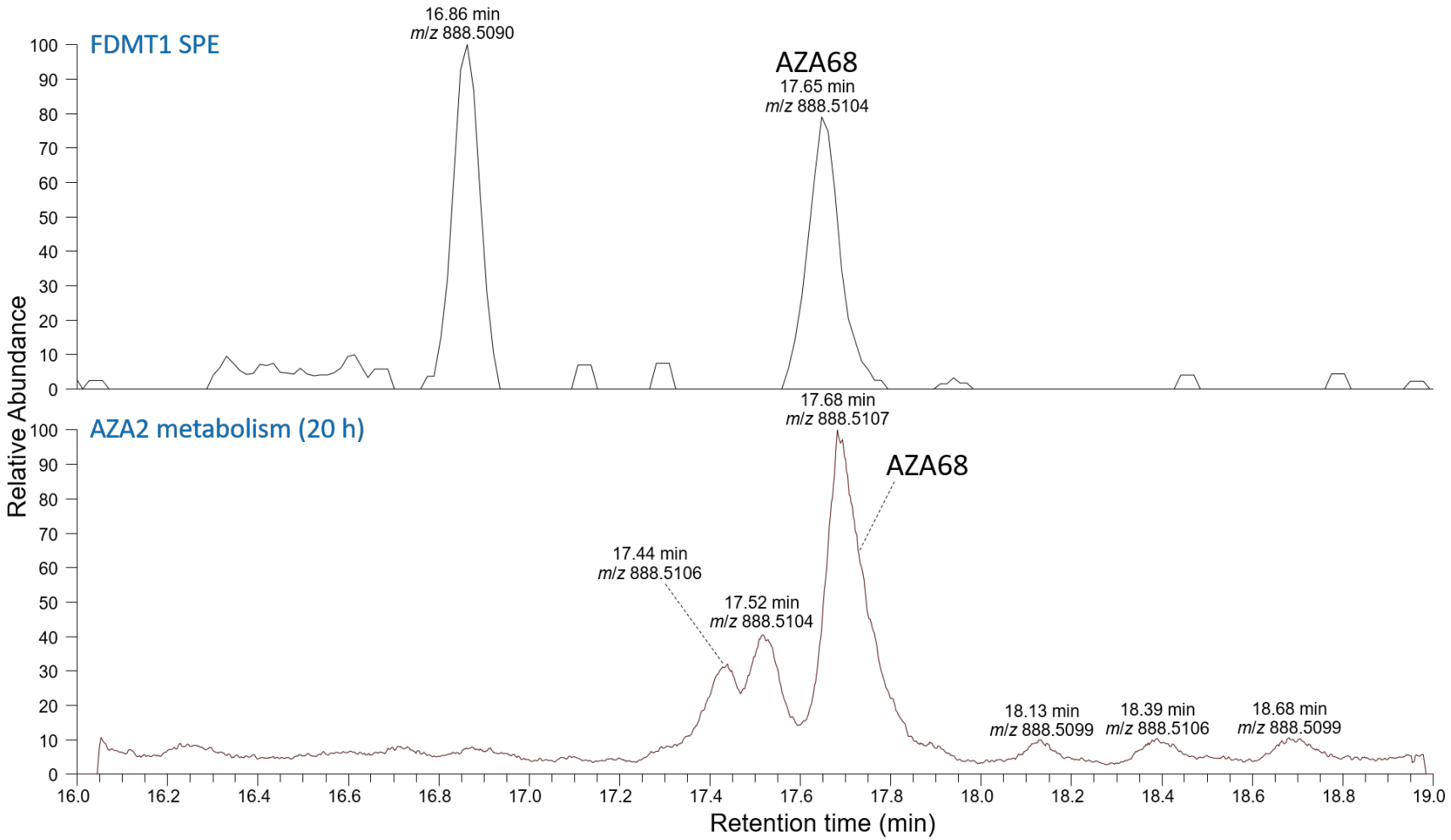

Figure S24. Extracted ion (*m/z* 888.5104 ±5 ppm) full-scan LC–HRMS (method B) chromatograms (16–19 min) of: top, an SPE-concentrated extract of NRC CRM-FDMT1 (Wright and McCarron, 2021), and; bottom, the AZA2 metabolism extract at 20 h. This confirms the presence of AZA68 in both the CRM-FDMT1 and AZA2 metabolism samples. The peak for AZA68 in FDMT1 SPE concentrate also displayed an appropriate HRMS/MS spectrum.

In vitro metabolism of AZA1–3 in blue mussel hepatopancreatic fraction

References

Kilcoyne, J., Twiner, M.J., McCarron, P., Crain, S., Giddings, S.D., Foley, B., Rise, F., Hess, P., Wilkins, A.L., Miles, C.O., 2015. Structure elucidation, relative LC–MS response and *in vitro* toxicity of azaspiracids 7–10 isolated from mussels (*Mytilus edulis*). J. Agric. Food Chem. 63, 5083−5091.

McCarron, P., Giddings, S.D., Reeves, K.L., Hess, P., Quilliam, M.A., 2015. A mussel (*Mytilus edulis*) tissue certified reference material for the marine biotoxins azaspiracids. Anal. Bioanal. Chem. 407, 2985−2996.

Wright, E.J., McCarron, P., 2021. A mussel tissue certified reference material for multiple phycotoxins. Part 5: profiling by liquid chromatography–high resolution mass spectrometry. Anal. Bioanal. Chem. 413, 2055−2069.